International Journal of Engineering Research and Development
e-ISSN: 2278-067X, p-ISSN: 2278-800X, www.ijerd.com
Volume 10, Issue 7 (July 2014), PP.34-41

Combustion Synthesis and Magnetic Studies of Hausmannite, Mn_3O_4, nanoparticles

J.S Sherin[1], J.K. Thomas[2*], J. Suthagar[3]
[1]*Department of Physics, Karunya University, Coimbatore*
[2]*Department of Physics, Electronic Materials Research Laboratory, Mar Ivanios college, University of Kerala*
[3]*Department of Engineering, Ibri College of Technology, Ibri, Sultanate of Oman*

Abstract:- Hausmannite, Mn_3O_4, nanoparticles were synthesized successfully via combustion synthesis route with $MnCl_2.4H_2O$ as manganese source. The samples were characterized to find the structural, functional and magnetic properties by XRD, FT-IR, FT-Raman and VSM respectively. An attempt is made to summarize the detailed field dependent magnetization study of the synthesized material is presented. Structural studies by XRD indicate that the synthesized material as tetragonal crystal structure with size 35nm. FT-IR and FT-Raman analysis revealed stretching vibrations of metal ions in tetrahedral and octahedral co-ordination confirming the crystal structure. Magnetic studies of the as synthesized sample depict paramagnetic behaviour at room temperature. The superparamagnetic behaviour was observed at room temperature with no saturation magnetization and hysteresis in the region of measured field strength. These measurements as a function of temperature and field strength showed a reduction in ferrimagnetic temperature T_c = 41K as compared to those reported for the bulk T_c = 43K.

Keywords:- A. Oxides, A. Nanostructure B. Chemical synthesis B. Magnetic properties

I. INTRODUCTION

A great deal of attention has paid to the synthesis of magnetic materials that have extensive applications in electronic and information technologies [1]. Magnetism of materials in the nanosize scale is of extreme importance due to their potential applications in different fields such as high density recording media, ferrofluid technology, magnetic resonance imaging etc [2-3]. When the crystalline sizes of magnetic material reduce to a few nanometres, energy considerations favour the formation of single domain particles which could exhibit unique properties such as superparamagnetism [4]. Recently, so far, most of the investigations of magnetic nanoscale materials have performed due to their unique physical properties arising from the quantum size effect, which makes them different from that of their bulk counterpart. The promising physical properties include changes in the Curie temperature, reduction in magnetic and presence of an enhanced anomalous magnetic hysteresis [5-7]. Magnetic nanostructured materials also have fascinated scientist as they are looking for perfect new materials from which future technologies can be built. Transition metal oxide components are showing considerable potential in this regard. Unlike ordinary metals, these materials cannot be understood by considering electrons that move independently from one another rather than electrons interact with each other strongly. This gives rise to exotic new magnetic and electronic properties, which can be exploited in new technologies [8-9].

Researchers have proposed several synthesis approaches such as co-precipitation [10], sol–gel [11], hydrothermal method [12], thermal decomposition [13], solvothermal method [14], microwave assisted method [15] and Combustion synthesis [16] for obtaining nanostructured materials. However, most of these approaches contain multi-step synthetic processes or protection from oxygen, involving unfavourably high growth temperatures and long reaction times. Currently, there is a trend towards simple, low temperature solution method for the nanoparticle preparation in order to yield desired particle size in nanocrystallinity. One of the novel and simple method for the synthesis of nanomaterials is the combustion technique in which nanocrystalline powders of oxide ceramics, metallic oxides, other inorganic oxides etc could be synthesised at lower calcinations temperature in a surprisingly short duration of time [17-19]. The combustion-synthesized powder also possesses high surface area and can be sintered to very high densities at relatively lower sintering temperatures. The powder properties can be systematically tuned by altering the oxidant to fuel ratio.

Over the past decade, magnetic nanoparticles of the 3d transition metal oxides have attracted enormous interest due to their potential applications in various fields ranging from catalysis, energy storage and magnetic data storage [20-22]. A large number of different manganese oxides are possible due to the availability of various oxidation states of manganese (II, III, IV). The most commonly known manganese oxides MnO, MnO_2, Mn_2O_3 and Mn_3O_4 have a wide range of applications in catalysis and battery technologies [23]. Among the

series of manganese oxides, Mn_3O_4 is known as an active catalyst in various oxidation and reduction reactions. Moreover, the catalystic application of Mn_3O_4 has been extended to the combustion of organic compounds at temperatures of the range of 373-773K [24-25].

Mn_3O_4 is a transition metal oxide with the normal spinel structure. The stable room temperature phase is tetragonal hausmannite ($14_1/amd$) with Mn^{3+} and Mn^{2+} occupying the octahedral (B-sites) and tetrahedral (A-sites) positions of the spinel structure respectively. The oxygen octahedral is tetragonally distorted due to Jahn-Teller effect on Mn^{3+} ions[26]. The ionic formula of Mn_3O_4 is usually written as $Mn^{2+}[Mn_2^{3+}]O_4$ corresponding to a normal spinel. However there are only few reports on the synthesis of Mn based nanoparticles and relating its magnetic characteristics with particle size. Due to the large number of applications of manganese oxides, the study of their nanoparticles is of great importance [27-28].

In this work, we present the synthesis of Mn_3O_4 nanopowder, using an auto igniting Combustion technique for the first time. The structural and vibrational characteristics are presented. A detailed field dependent magnetization study of the synthesized material is also presented.

II. EXPERIMENTAL ANALYSIS

2.1 Synthesis of nanopowders

A modified auto – igniting solution combustion technique, was used for the synthesis of nanoparticles of Mn_3O_4. In the typical synthesis, aqueous solution containing ions of Mn was prepared by dissolving stoichiometric amount of high purity $MnCl_2.4H_2O$ in double distilled water (200 ml) in a beaker. Citric acid (99%) was then added to the solution containing Mn ions. Amount of Citric acid was calculated based on total valence of oxidising and the reducing agents for maximum release of energy during combustion. Oxidant/Fuel ratio of the system was adjusted by adding nitric acid and ammonium hydroxide and the ratio was at unity. The solution containing the precursor mixture was heated using a hot plate at 250 ^{0}C in a ventilated fume hood. The solution boils on heating and undergoes dehydration accompanied by foam. The foam then ignites by itself on persistant heating giving voluminous and fluffy greyish black product on combustion. The combustion product was calcinated at about 923 ^{0}C for 1 hour. The final powder was collected for characterization and subsequently characterised as single-phase nanocrystals of Mn_3O_4.

2.2 Characterization.

The structure of the as-prepared nanopowders were characterized by XRD (XPERT – PRO) diffractometer using Cu k_α radiation source (1.5406 nm) at 40 KV and 30 mA in the region $20^0 – 90^0$ with 0.084 step size (and continuous scanning). Fourier transform infrared (FT-IR) spectra were recorded in transmission mode using a Thermo Nicolet, Avatar 370 FT-IR Infrared spectrometer. The powder samples were ground with KBr and compressed into a pellet. FT-IR spectra in the range 4000 – 400 cm^{-1} with a spectral resolution of 4 cm^{-1} were recorded in order to investigate the nature of chemical bonds of specific functional groups formed. Fourier transform Raman spectra were recorded using Bruker RFS Stand alone FT-Raman Spectrometer. The spectral range is 1000 – 200 cm^{-1} with a resolution of 2cm^{-1} and the source is Nd: YAG laser with a wavelength 1064 nm. VSM measurements were performed by using a Quantum Design Vibrating sample magnetometer. The sample was measured between 1KOe – 15KOe at room temperature and at 10K. ZFC (zero field cooling) and FC (field cooling) measurements were carried out at 100 Oe and the blocking temperature was determined from the measurements.

III. RESULTS AND DISCUSSION

3.1 XRD analysis

X-ray powder diffraction (XRD) analysis was used to determine the phase of the sample. Figure 1 shows the XRD pattern of the synthesised material where all the diffraction peaks in the pattern can be indexed to tetragonal Mn_3O_4 (JCPDS card No 24-0734) with space group $I4_1/amd$ (141). All the peaks in the pattern can be readily indexed to a tetragonal phase of Mn_3O_4 with lattice constants a = 5.7085 ^{o}A and c = 9.30656 ^{o}A, which are in good agreement with the reported data (a = 5.7621 ^{o}A and c = 9.4696 ^{o}A). The crystallite size is deduced from Debye – Scherrer formula,

$$D = k\lambda/\beta Cos\theta$$

where β is the broadening of diffraction line measured at half of its maximum intensity and k is a constant.

The calculated average crystallite size was 35nm. No peaks of any other phases are detected, indicating the purity of the final product. The strong and sharp reflection peaks suggest that the as-prepared nanopowders are well crystallised. The XRD pattern of the nano powder showed that they were predominantly composed of BCC Mn_3O_4.

3.2 FTIR Analysis

The FT-IR analysis of the as-prepared samples were performed and the spectrum is shown in figure 2. The vibrational spectrum of as-prepared Mn_3O_4 nanoparticles without any thermal treatment displays two significant absorption bands in the range of 400 – 700 cm^{-1}, where stretching and bending vibrations of MnO_n units are showing up [29]. The vibrational frequency located at 613 cm^{-1} is the characteristic of Mn–O stretching modes in tetrahedral sites. The second vibrational band, located at 491 cm^{-1} , can be attributed to the vibration of manganese species (Mn^{3+}–O) in the octahedral site of Mn_3O_4 [30–31]. These absorption peaks may be associated with the coupling mode between the Mn-O stretching modes of the tetrahedral and octahedral sites. This confirms the formation of the manganese oxide compound.

Moreover, the bands between 3500 cm^{-1} and 1500 cm^{-1} could be assigned to the O–H vibration of the weakly bonded physisorbed water molecules. A broad band at around 3426 cm^{-1} were caused by the stretching vibrations of the O-----H bond and other weak band at 1616 cm^{-1} were due to the bending vibrations of O---H molecules. The peaks at 1038 cm^{-1} and 962 cm^{-1} were attributed to the O—H bending modes respectively to γ-OH and δ-2 OH [32]. Thus, the FT-IR spectrum provides concrete evidence for the formation of Mn_3O_4 nanopowder.

3.3 FT- Raman Analysis

The Hausmannite Mn_3O_4 ($MnMn_2O_4$ in spinel notation) is a normal tetragonal spinel structure with space group $14_1/amd$. Factor group analysis performed by the correlation method gives 14 Raman active modes with $\Gamma = 2A_{1g} + 2B_{1g} + 4B_{2g} + 6E_g$. Raman spectra of hausmannite Mn_3O_4 sample is shown in the figure 3. The Raman spectrum displays sharp peaks in the range of 200 – 1000 cm^{-1}. The small peaks at 860, 804, 749 and 708 cm^{-1} display resolved and sharp bands of Mn-O bending vibrations.

The Raman spectrum of Mn_3O_4 is characterised by a very sharp peak at 654cm^{-1}, which was found on mineral Hausmannite, as well as on either chemically prepared sample. This peak is characteristic of all the spinel structure and other manganese oxides where the vibration involves the motion of oxygen inside the octahedral unit MnO_6. In particular the mode at 654cm^{-1} has been considered as A_{1g} symmetry that corresponds to Mn-O stretching vibration. Four smaller peaks are observed between 420-570 cm^{-1} i.e., 358, 428, 465 and 559 cm^{-1} are the wavenumber modes which involve mainly due to the displacement of oxide ions, although the vibrations are attributed to the Mn-O stretching mode [33-34]. These Raman spectra features are in good agreement with the literature data. Raman spectral analysis corroborates with the XRD results confirming the formation of Mn_3O_4 during Combustion.

3.4 Vibrating Sample Magnetometry Analysis

The magnetic property of the Mn_3O_4 nanoparticles were investigated by measuring the magnetization in both zero field cooled (ZFC) and field cooled (FC) modes under 100 Oe magnetic field. It is revealed that the magnetization decreases by increasing the temperature upto 41K and then sharply decreases around 43K. The magnetization almost disappears above 44K. The ZFC and FC curves coincide initially and start to deviate from each other and follow different paths as the temperature is decreased from 200K to 10K. The shape of ZFC and FC is the result of dipole-dipole interaction between Mn_3O_4 nanoparticles. As shown in the figure 4, the variation of magnetization in ZFC and FC mode indicates the superparamagnetic behaviour. ZFC measurement was carried out as the temperature is decreasing from room temperature to 10 K without the application of external magnetic field.

In both ZFC and FC curves, the magnetization starts to increase sharply with decreasing temperature and the sample shows the existence of magnetic moments with and without the field. It changes its magnetic characteristics at this temperature is known as Curie temperature, T_c. The measure T_c for Mn_3O_4 nanoparticles of size 19nm is 42 K. Both Winkler et al [35] and Regmi et al [36] reported that T_c to be 42 K for Mn_3O_4 nanoparticles with average size of 15 nm in different studies, which is in consistency with our observations. A detailed description about the varying magnetic transition temperature for Mn_3O_4 with the particle size in the range of 15 – 30 nm can be found in [36]. The transition temperature can be determined through the derivative of magnetizations with respect to the temperature. The transition temperature was found at 40 K, which is lower than the observed temperature for the bulk of Mn_3O_4 (43 K). A blocking temperature T_B of 40 K was observed comparable to that reported by Seo et al [37] for 10 nm Mn_3O_4 spherical nanoparticles. As the temperature decreases the deviation between ZFC and FC curves starts at about blocking temperature, (T_B) 40.9 K.

In the temperature range from 0 to 80 K, the magnetizationvalue is a constant near to zero, which shows the excellent paramagnetic behaviour of the product. Mn_3O_4 nanostructure shows ferrimagnetic behaviour at low temperatures where the T_c for the samples was found at 40 K and 42 K. In comparison, it has been reported that Mn_3O_4 has a Curie temperature of 41 K [38].

The magnetization curve of Mn3O4 sample prepared using the present combustion technique at 10K and 15K is shown in figure 5(a) and 5(b) respectively.

The hysteresis loop was obtained in a magnetic field of upto ± 15 KOe. The saturation magnetization was not reached, showing a maximum magnetization, (M_{max}) about 22.67 emu/g at 10 K, which is smaller than the saturation magnetization of Mn_3O_4 in coarse-grained form. This value represents the 60% of the saturation magnetization of the bulk Mn_3O_4 M_{max} = 38 emu/g. A remanence ratio (M_r/M_{max}) of 0.78 was estimated from the remanence value (M_r) of 17.775emu/g. The coercivity (H_c) of the as-synthesized nanopowder was of 1.156 kOe. The smaller M_s values in nanoparticles are generally attributed to the core shell structure with aligned moments in core and canted surface moments reducing magnetization. A principle effect of this finite size is the breaking of a large number of bonds on the surface. Then, the surface cations produce a core of aligned spins surrounded by a disordered shell. This can result in a disordered spin configuration near to the surface and a reduced average net moment compared to the bulk materials [39 – 40]. In addition, the surface spin states can result in high field hysteresis and relaxation of the magnetization. Moreover, non-saturated magnetization at hysteresis means a co-existence of antiferromagnetic interactions with ferromagnetic interaction at low temperatures. All hysteresis show a small amount of coercive field and this asymmetry increases with decreasing temperature.

IV. CONCLUSION

In summary, a simple auto igniting combustion method has been used to successfully prepare Mn_3O_4 nanoparticles, which are indexed as tetragonal hausmannite. As synthesized Mn_3O_4 nanoparticle have been identified using XRD analysis were proven to be single crystal in nature with average particle size of 35nm. Functional studies were carried out using FT-Raman and FT-IR. FT-Raman analysis showed the characteristic peak which was found on mineral hausmannite. FT-IR analysis revealed stretching vibrations of metal ions in tetrahedral and octahedral co-ordination confirming the crystal structure. Various bending and stretching modes of Mn-O groups were analysed from the spectroscopic studies. The convenience of the process,good reproducibility for the present method make it possible to scale up. The magnetic measurements of the as-synthesized Mn_3O_4 nanoparticles revealed that the blocking temperature, T_c of 41K, above which the material behaves as paramagnetic. This agrees with the bulk material value whereas the remnant magnetization and coercivity are 17.775emu/g and 1156 Oe respectively. Such magnetic properties hint at several interesting prospects for future studies. This combustion route can be considered as an economical and facile approach to prepare Mn_3O_4 nanoparticle.

ACKNOWLEDGMENTS

We are thankful to the Department of Physics, Karunya University Coimbatore and Electronic Materials Research Laboratory of Mar Ivanios College for their experimental facilities.

REFERENCES

[1]. E. Grootendorst, Y. Verbeek, V. Ponce, J. Catal. 706 – 712 (1995) 157.
[2]. H. Gleiter, Acta. Mater. 1-29 (2000) 48.
[3]. M.C. Bernard, H.L. Goff, B.V. Thi, J. Elect. Chem. Soc. 3065 (1993) 140.
[4]. A.H. De Vries, L. Hozoi, R. Broer, Phys. Rev. B 035108 (2002) 66.
[5]. W.S. Kijlstra, J. Daamen, J.M. Vandegraaf, B. Vanderlinden, E.K. Poels, A. Bliek, Appl. Catal. B: Environ. 337 (1996) 7.
[6]. M.P.M. Dean, Nat. Mater. 850-854 (2012) 11.
[7]. M.H. Kryder, MRS Bull. 17 (1996) 21.
[8]. M.E. McHenry, D.E. Laughlin, Acta. Mater. 223 (2000) 48.
[9]. H. Gleiter, Prog. Mater. Sci. 223 (1989) 33.
[10]. B.D. Cullity, Introduction to Magnetic Materials, Addison-Wesley, Reading, MA, USA, (1972).
[11]. L. Chen, T. Horiuchi, T. Mori, Appl. Catal. A: Gen. 97 (2001) 209 E.R. Stobhe, B.A.D. Boer, J.W. Geus, Catal. Today 161 (1999) 47.
[12]. Y.Q. Chang, X.Y. Xu, X.H. Luo, C.P. Chen, D.P. Yu, J. Cryst. Growth 232 (2004) 264.
[13]. K.S. Suslick, S.B. Choe, A.A. Cichowalas, M.W. Grinsta, Nature 414 (1991) 353.
[14]. A. Gedanken, Ultrson. Sono. Chem. 47 (2004) 11.
[15]. J. Koshy, J. K. Thomas, J. Kurian, Y. P. Yadav, A. D. Damodaran U.S. Patent No. 5856276, Jan 5, (1999).
[16]. J. Koshy, J. K. Thomas, J. Kurian, Y. P. Yadav, A. D. Damodaran, Ceramic substrates
[17]. for superconducting films, European Patent No. EP 0679615 B1, 21 July, (1999).
[18]. J. James, R. Jose, A. M. John, J. Koshy, US Patent No. 6761866, July 13, (2004).
[19]. J. James, R. Jose, A. M. John, J. Koshy, US Patent No. 6835367, Dec. 28, (2004).
[20]. A.R. Armstrong, P.G. Bruce, Nature, 499-500 (1996) 381.

[21]. A. H. De Vries, L.Hozoi, R. Broer, Phys. Rev. B 035108 (2002) 66.
[22]. Y. C. Zhang, T. Qiao, X. Y. Hu, J. Solid State Chem. 4093-7 (2004) 177
[23]. O. Giraldo, S.L, Brock, M. Marquez, J. Am. Chem. Soc.9330 (2000) 122.
[24]. M. Baldi, E. Finochhio, F. Milella, G. Busea, Appl. Catal. B 43 (1998) 16.
[25]. M.F.M. Zwinkels, S.G. Jaras, P.G. Menon, T.A. Griffik, Catal. Rev.Sci. Eng., 319 (1993) 35.
[26]. O.Y. Gorbenko, Solid State Commun. 15 (2002) 124.
[27]. B. Boucher, R. Buhl, M. Perrin, J. Appl. Phys. 1615 (1971) 42.
[28]. K. Dwight, N. Menyuk, Phys. Rev. 1470 (1960) 119.
[29]. P.K. Sharma, M.S. Whittingham, Mater. Lett. 319 (2001) 48.
[30]. Pierre Gibot, Lydia Laffont, J. Solid State Chem.180 (2007) 695.
[31]. D.P. Dubal, Dhawale, T.P. Gujar, C.D. Lokhande, Appl. Surface Sci. 257 (2011) 3378.
[32]. Brian Smith, Infrared Spectral Interpretation: A Systematic Approach, First ed., CRC press, (1999).
[33]. Yong Cai Zhang, Tao Qiao, Xiao Ya Hu, J. Solid State Chem. 177 (2004) 4093.
[34]. J.D. Dunitz, L.E. Orgel, J. Phys. Chem. Solid 3 (1957) 318.
[35]. E. Winkler, R.D. Zyster, D. Fiorani, Phy. Rev. B 70 (2004) 174406.
[36]. R. Regmi, R. Tackett, G. Lawes, J.Magn.Mater., 321 (2009) 2296.
[37]. W.S Seo, H.H. Joe, B. Kim, J.T, Park, Angew. Chem. Int. Ed, 43 (2004) 1115-1117.
[38]. S. Krupichka, Physik der Ferrite und der Magnetiscen Oxide, Academia Verlag, Prague,(1973).
[39]. S. Tikadzumi, Physics of Ferromagnetism, Magnetic Characteristics and Practical Use, Mir, Moscow (1987).
[40]. A. Baykal, H. Kavas, Z Durmus, M. Demir, S. Kazan, R. Topkaya, M.S.Toprak, Cent. Eur. J. Chem., 83 (2010) 633-638.

FIGURE OPTIONS

Figure: 1 XRD image of Mn_3O_4 nanoparticles.
Figure: 2 FT-IR spectra of as synthesized Mn_3O_4 nanoparticle.
Figure: 3 FT-Raman spectra of Mn_3O_4 nanoparticles.
Figure: 4 ZFC and FC magnetization curves of Mn_3O_4 nanopowder under an applied field of 100 Oe.
Figure: 5a Magnetic hysteresis loop at 10K.
Figure: 5b Magnetic hysteresis loop at 15K.

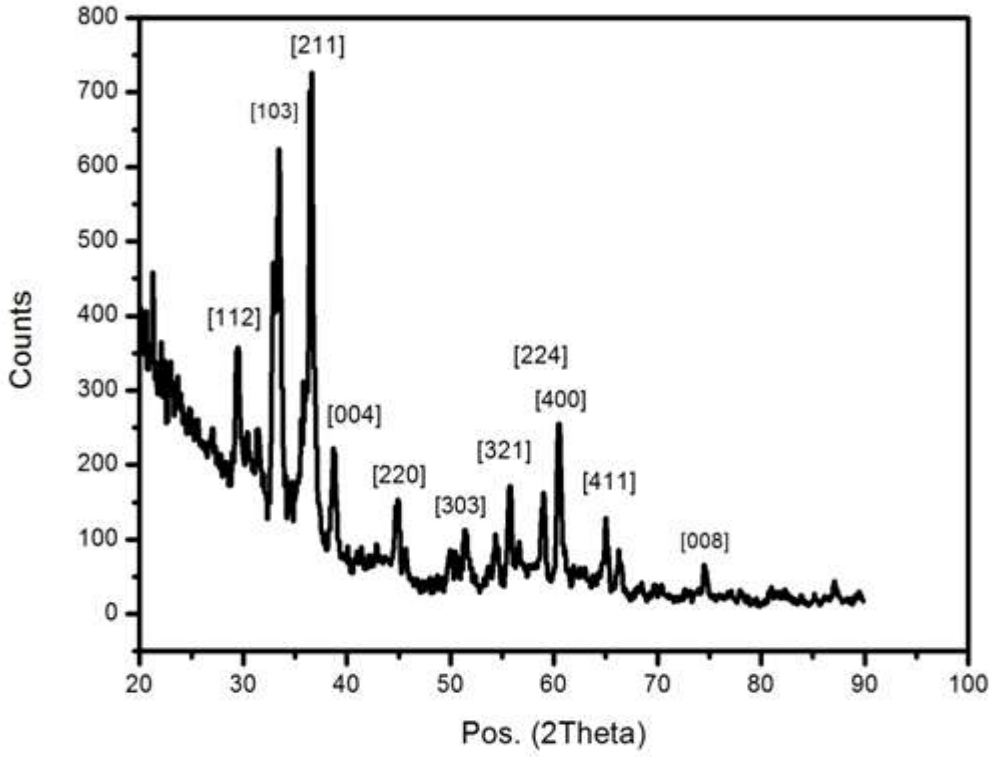

Figure 1

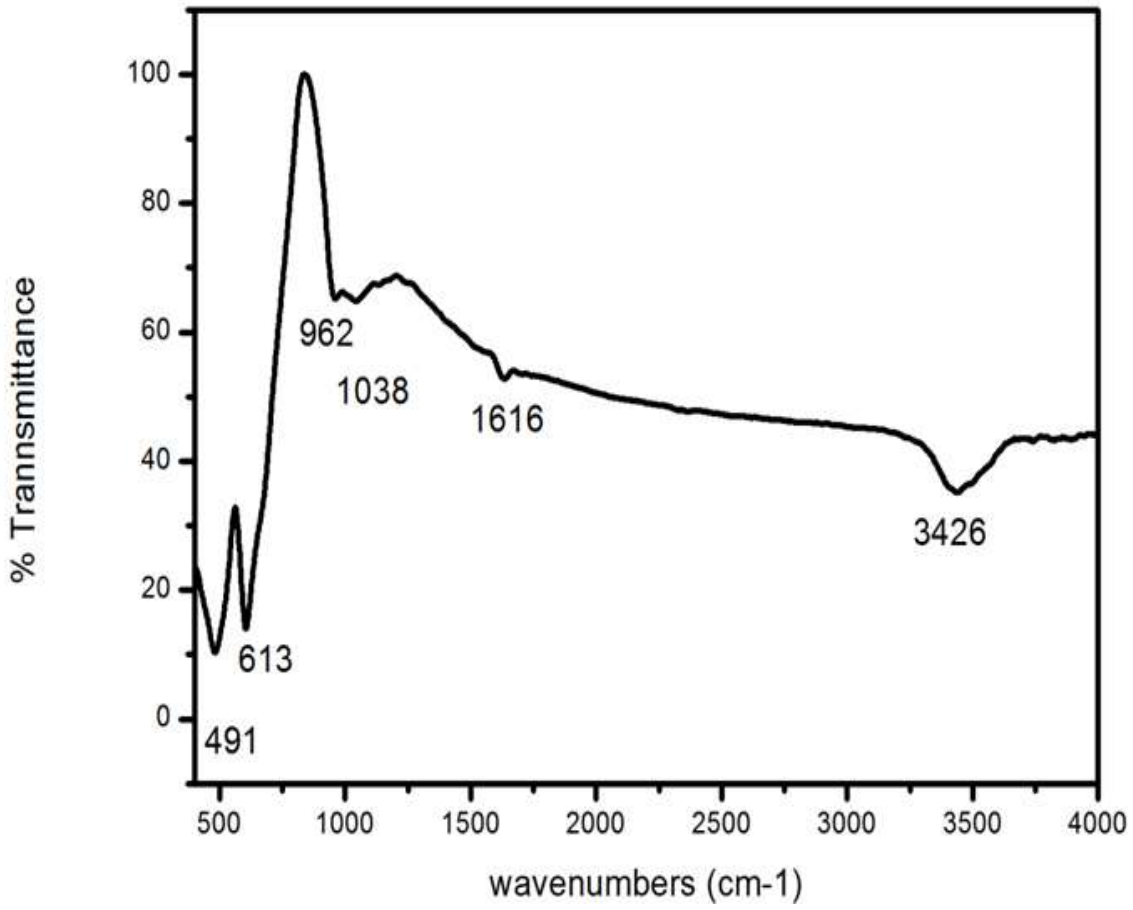

Figure 2

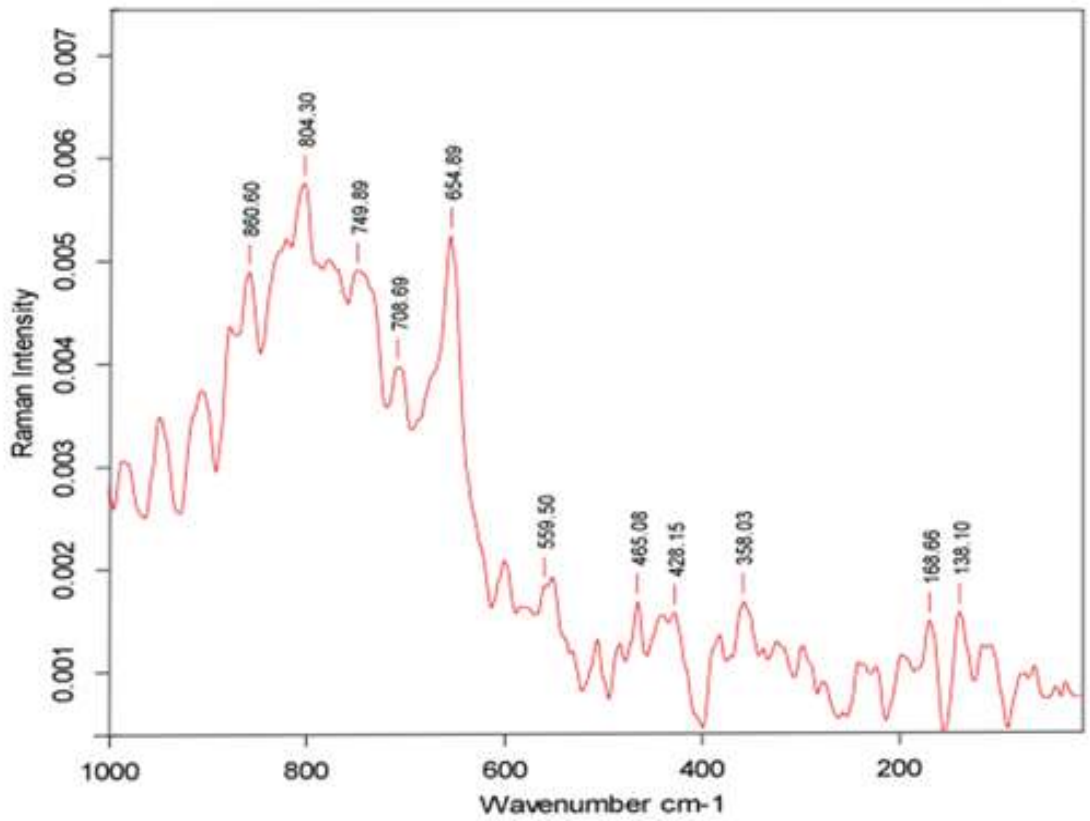

Figure 3

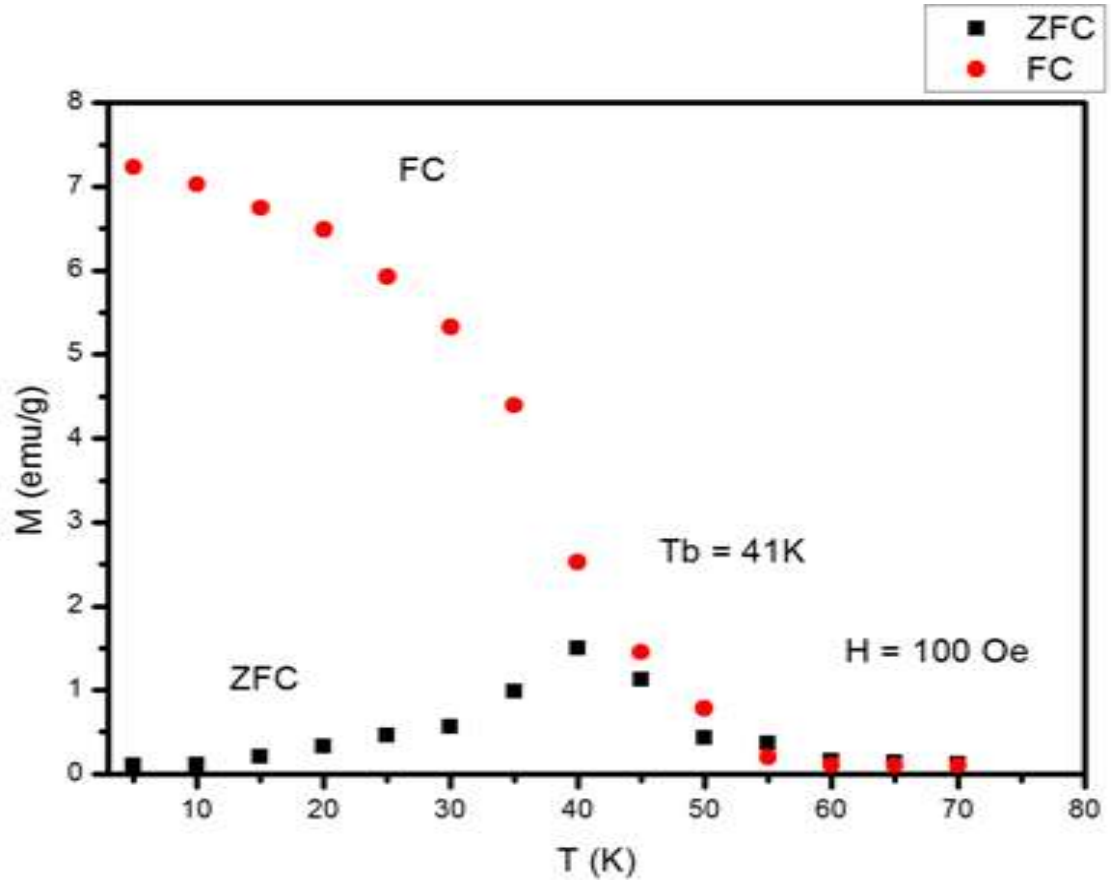

Figure 4

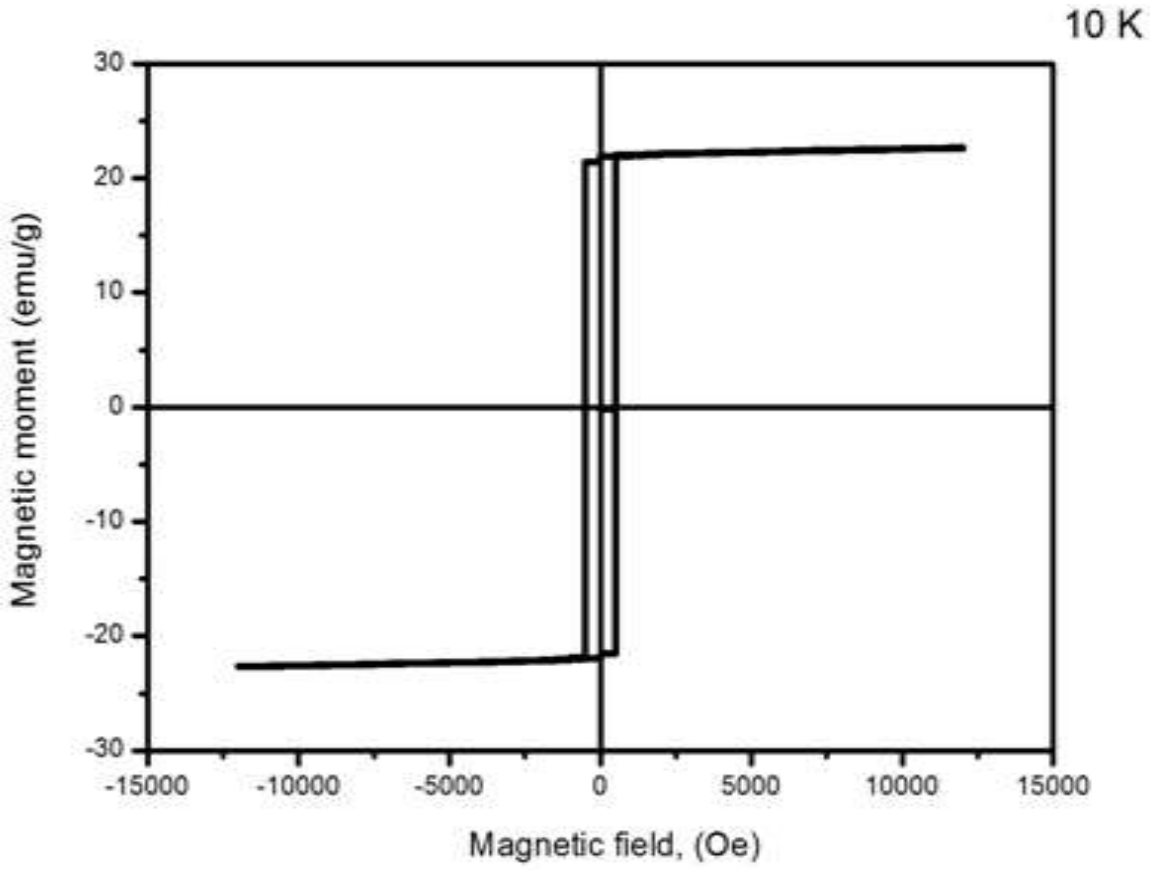

Figure 5

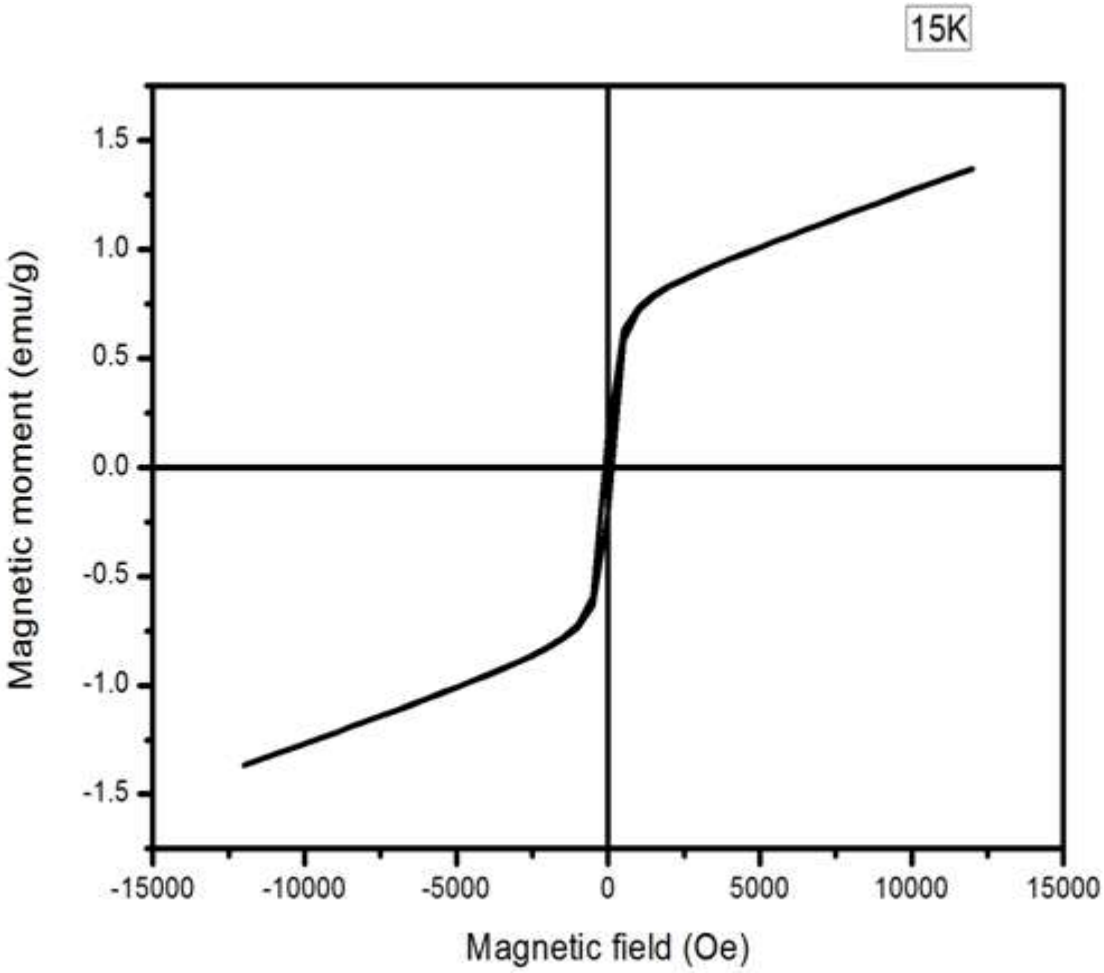
15K
Magnetic moment (emu/g)
1.5
1.0
0.5
0.0
-0.5
-1.0
-1.5
-15000
-10000
-5000
0
5000
10000
15000
Magnetic field (Oe)

Figure 6